



**HAL**  
open science

# A Flow Time Model for Melt-Cast Insensitive Explosive Process

Jean-Philippe Guillemin, Luc Brunet, Olivier Bonnefoy, Gérard Thomas

► **To cite this version:**

Jean-Philippe Guillemin, Luc Brunet, Olivier Bonnefoy, Gérard Thomas. A Flow Time Model for Melt-Cast Insensitive Explosive Process. XI<sup>e</sup> Congrès de la Société Française de Génie des Procédés. Des réponses industrielles pour une société en mutation., Oct 2007, Saint Etienne, France. pp.ISBN=2-910239-70-5. hal-00457829

**HAL Id: hal-00457829**

**<https://hal.science/hal-00457829>**

Submitted on 18 Feb 2010

**HAL** is a multi-disciplinary open access archive for the deposit and dissemination of scientific research documents, whether they are published or not. The documents may come from teaching and research institutions in France or abroad, or from public or private research centers.

L'archive ouverte pluridisciplinaire **HAL**, est destinée au dépôt et à la diffusion de documents scientifiques de niveau recherche, publiés ou non, émanant des établissements d'enseignement et de recherche français ou étrangers, des laboratoires publics ou privés.

## **A Flow Time Model for Melt-Cast Insensitive Explosive Process**

**GUILLEMIN JEAN-PHILIPPE<sup>(1)\*</sup>, BRUNET LUC<sup>(2)</sup>, BONNEFOY OLIVIER<sup>(1)†</sup>, THOMAS GÉRARD<sup>(1)</sup>**

*(1) Ecole Nationale Supérieure des Mines de Saint-Etienne, Centre SPIN, Département PMMC, LPMG UMR 5148, 158 Cours Fauriel 42023 Saint-Etienne Cedex 2, France*

*(2) Nexter Munitions 7, route de Guerry, 18023 Bourges Cedex (France)*

### **Abstract**

Diphasic flows of concentrated suspensions of melt-cast insensitive explosives exhibit particular rheology properties. In order to limit the handling of pyrotechnical products presenting a risk with respect to the mechanical and thermal shocks, a lot of works have been undertaken for many years in the civil engineering sector. The objective of this study is to propose a predictive model of the flow time of a concentrated suspension through a nozzle located at the bottom of a tank. Similarly to our industrial process, the suspension is made out of insensitive energetic materials and flows under gravity. Experimental results are compared to three models (Quemada, Krieger-Dougherty, and Mooney) predicting the viscosity  $\mu$  of a suspension as a function of the solid volume fraction  $\phi$ , the maximum packing density  $\phi_m$  and the viscosity  $\mu_0$  of the interstitial liquid. De Larrard's model is used to calculate  $\phi_m$ . The value of viscosity measured for the pure liquid is near the one predicted by the Bernoulli theorem, where liquids are considered as incompressible and perfect. In the end, it turns out that the Quemada's model gives a fair agreement between predictions and experiments.

### **Keywords:**

*Melt-Cast Insensitive Explosive ; Flow Time Model ; Maximum Packing Density ; De Larrard's Model.*

### **I. Introduction**

The purpose of this article is to propose a predictive model of the flow time necessary for emptying a reactor filled with a concentrated suspension through a nozzle situated at the bottom. Similarly to our industrial process, the suspension is made out of insensitive energetic materials and flows under gravity. Experimental results are compared with three viscosity models largely used in the field of concentrated suspensions (Quemada, 1977; Krieger and Dougherty, 1959; Mooney, 1951). These models give the dynamic viscosity of a concentrated suspension as a function of the viscosity  $\mu_0$  of the pure liquid, the volume fraction  $\phi$  of the solid included in the paste, and the maximum packing density  $\phi_m$ . These parameters will be used as a basis to establish our model. First, a relationship between the viscous and flow time terms starting from Navier-Stokes equation is needed. Secondly, evaluations of some characteristics of the granular phase in concentrated suspensions will be obtained and inserted in our flow time equations. With solid volume fractions higher than 50% and different morphologies and sizes, insensitive energetic materials carried out by melt cast process nicely compare with fresh concretes. So calculations of granular arrangements will be developed with scientific tools used satisfactorily in the civil engineering sector (Ferraris, 1999; De Larrard *et al.*, 1998; Shilstone, 1990. In particular the De Larrard's model for the calculation of the maximum packing density  $\phi_m$  (De Larrard *et al.*, 1998) will be considered.

---

\* Corresponding Author: [jp.guillemin@gmail.com](mailto:jp.guillemin@gmail.com)

† Corresponding Author: [obonnefoy@emse.fr](mailto:obonnefoy@emse.fr)

The study of the dependence of the casting time upon weak variations of the formulation and upon the choice of raw materials will make possible to compare the experimental results and those given by our model.

Melt casting energetic formulations are established for use in a cylindrical tank of a total volume of 5700 cm<sup>3</sup>. The experiments for flow time determinations are all performed in this container.

## II. Model description

### II.1 Rheology of Concentrated Suspensions

Since the publication of Einstein analysing the viscosity of dilute suspensions of rigid spheres in a viscous liquid, numerous equations have been developed to try and extend Einstein's formula to suspensions of higher concentrations (Teipel, 2005). The various resulting formulas differ considerably from each other. In this study, three relationships have been selected to express the dynamic viscosity of dispersions of spherical particles as a function of the dynamic viscosity of the interstitial fluid  $\mu_0$ , the volume fraction of solids  $\phi$  and the maximum packing density of the solids  $\phi_m$ . Others equations are given in the literature, but the three retained hereafter seem to be the most encountered, discussed and reliable, and this is the reason why they have been chosen in this study. These equations are given in Table 1.

*Table 1. Rheological equations*

Authors	Rheological equations
Krieger-Dougherty [2]	$\mu = \mu_0 \left(1 - \frac{\phi}{\phi_m}\right)^{-2.5\phi}$
Quemada [1]	$\mu = \mu_0 \left(1 - \frac{\phi}{\phi_m}\right)^{-2}$
Mooney [3]	$\mu = \mu_0 \exp\left(\frac{2.5\phi}{1 - \frac{\phi}{\phi_m}}\right)$

### II.2 Model

#### II.2.1 Relationship between Dynamic Viscosity and Flow Time

Because of the high solid content and the low flow velocity, it is assumed here that Reynolds number is not too important, although greater than unity. The inertial term of the Navier-Stokes equation is supposed to be small enough with respect to the viscous term. The momentum equation takes the following simplified form:

$$\rho \cdot \frac{\partial \vec{v}}{\partial t} = -\vec{\nabla} p + \mu \cdot \Delta \vec{v} + \rho \cdot \vec{g} \quad (1)$$

As the suspension flows during a relatively long time (over one minute), the state can be regarded as quasi-stationary and one can write at any time:

$$\mu \cdot \Delta \vec{v} = \vec{\nabla} p - \rho \cdot \vec{g} \quad (2)$$

Equation 2 implies that, for a given pressure gradient, the flow rate of a fluid is inversely proportional to its viscosity. This can be applied to the two fluids considered, the suspension with a viscosity  $\mu$  and the interstitial fluid with a viscosity  $\mu_0$ . Therefore, for a given volume, the flow time  $\tau$  is directly proportional to the viscosity:

$$\frac{\tau}{\tau_0} = \frac{\mu}{\mu_0} \quad (3)$$

Where  $\tau_0$  represents the flow time for the interstitial fluid.

*II.2.2 Calculation of  $\tau_0$  by Bernoulli's approach*

The interstitial fluid is a mixture of trinitrotoluene TNT and additives, presenting viscosities of 11 and 48.6 mPa.s respectively. Such values are rather small, and the interstitial fluid can be assimilated to a perfect fluid: this allows us to use the Bernoulli relationship in the tank described on Figure 1.

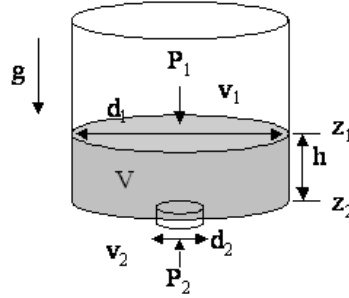


*Figure 1. Tank geometry*

Where  $V$  [m<sup>3</sup>] is the suspension volume;  $v_1$  and  $v_2$  [m/s] are the fluid velocities;  $P_1$  and  $P_2$  [Pa] are the top and bottom pressures;  $d_1$  and  $d_2$  [m] are the diameters of sections 1 and 2;  $h = z_1 - z_2$  [m] is the fluid height;  $g$  [m/s<sup>2</sup>] is the acceleration of gravity equal to 9.81 m/s<sup>2</sup>.

The Bernoulli relationship can be written:

$$\frac{\rho v_1^2}{2} + P_1 + \rho g z_1 = \frac{\rho v_2^2}{2} + P_2 + \rho g z_2 \quad (4)$$

Where  $\rho$  represents the fluid density [kg/m<sup>3</sup>].

The mass balance gives:

$$v_1 d_1^2 = v_2 d_2^2 \quad (5)$$

With  $v_1 = -dh/dt$ , so that Equation (4) could be written now:

$$\frac{dh}{dt} = \sqrt{\left(\frac{a \cdot (h+b)}{c}\right)} \quad (6)$$

Where  $a = 2g$ ;  $b = (P_1 - P_2)/(\rho g)$ ;  $c = (d_1/d_2)^4 - 1$

The integration of Equation (6) between  $t=0$  and  $t=\tau$ , where the liquid heights are respectively  $h_0$  and  $h(\tau)$  leads to Equation 7:

$$\sqrt{h(\tau)+b} = \sqrt{h_0+b} - \tau \sqrt{\frac{a}{4 \cdot c}} \quad (7)$$

At  $\tau_0$ , the tank is empty and  $h(\tau_0)=0$ . Finally,  $\tau_0$  is given by Equation 8

$$\tau_0 = \sqrt{\left(\frac{d_1}{d_2}\right)^4 - 1} \cdot \sqrt{\left(\frac{2}{g}\right)} \cdot \left[ \sqrt{h_0 + \frac{(P_1 - P_2)}{\rho g}} - \sqrt{\frac{(P_1 - P_2)}{\rho g}} \right] \quad (8)$$

With Equations 3 and 8 and one of the rheological equations given in Table 1, three relationships, Equations 9, 10 and 11 allow us to calculate the flow time for our energetic concentrated suspensions. These relationships depend on the solid volume fraction  $\phi$ , the flow for the interstitial fluid  $\tau_0$  and the maximum packing density  $\phi_m$ .

$$\tau = \tau_0 \left( 1 - \frac{\phi}{\phi_m} \right)^{-2.5\phi_m} \quad (9)$$

$$\tau = \tau_0 \left( 1 - \frac{\phi}{\phi_m} \right)^{-2} \quad (10)$$

$$\tau = \tau_0 \exp \left( \frac{2.5\phi}{1 - \frac{\phi}{\phi_m}} \right) \quad (11)$$

### II.2.3 Calculation of the Maximum Packing Density

Many studies aim at improving predictions of viscosity by refining the methods of calculation of the maximum packing density (Toutou *et al.*, 2004; Gan *et al.*, 2004; Stroeven, 2003). Many strong similarities appear between concrete and explosive made by casting process as the great number of granulometric scales, and the range of the component morphologies. In this kind of approach, the model developed by De Larrard seems very attractive (De Larrard and Sedran, 2002). This model predicts the maximum packing density of a polydisperse mix, from three parameters: the particle size distribution of the mix, its true density and the experimental packing density of the solid species. The use of software is required to determine the maximum packing density. In this study, the RENE-LCPC software developed by De Larrard and T. Sedran (Sedran and De Larrard, 1994) has been selected. The details of the algorithm will not be described here but the interested reader may refer to some of the associated publications (Stovall *et al.*, 1986; De Larrard, 1967; De Larrard, 1992). This model deals with grain mixtures in which linear combinations of packing densities allow to predict the packing density of a mixture of monosized particles  $d_i$  ( $d_1 < d_2 < \dots < d_n$ ) from:

$$\phi_i = \frac{\beta_i}{1 - (1 - \beta_i) \sum_{j=1}^{i-1} a_{ij} \alpha_j - \sum_{j=i+1}^N b_{ij} \alpha_j} \quad (12)$$

Where  $\phi_i$  is the packing density of class  $i$ ;  $\alpha_i$  is the volume fraction of belonging to class  $i$ ;  $\beta_i$  is the residual packing density *i.e.* when the class  $i$  is alone and fully packed. To compute the packing density of the overall mixture, one considers that the bulk volume of the class  $i$  fills the porous space around the coarser grains; moreover, the volume of finer classes inserted in the voids of class  $i$  must be added. Two interaction effects must be taken into account in this calculation: the wall effect,  $a_{ij}$ , exerted by the coarser particles and the loosening effect,  $b_{ij}$ , exerted by the finer particles. Finally,  $\phi_m$  is given by Equation 13.

$$\phi_m = \min_{1 < i < N} \phi_i \quad (13)$$

## III. Raw Materials and Experimental Set-up

### III.1 Raw Materials

The compounds used in this study are listed in Table 2.

Table 2. Studied compounds

Compounds	Name	True Density (g/cm <sup>3</sup> )	Melting Point (°C)	Physical state at exp. Conditions
TNT	2,4,6-trinitrotoluene	1.65	81	liquid
A	Additive	1	83	liquid
Al	Aluminium	2.7	660	solid
NTO	3-nitro-1,2,4-triazol-5-one	1.92	279	solid

### III.1.1 Rheology of the Liquid Phase

The liquid phase is composed of TNT and a fusible additive A. The dynamic viscosity of the additive is measured by a viscometer presenting a “Couette” geometry (Rheomat 30, Contrave). A thermo-regulated bath is used to control the temperature. Results show that the additive has a newtonian behaviour and its dynamic viscosity is equal to 48.6 mPa.s at 85°C. The TNT dynamic viscosity  $\mu_{TNT}$  is calculated with Equation (14) established by (Parry and Billon, 1988) on temperature as follows:

$$\mu_{TNT} = \mu^* \exp\left(\frac{Q}{T}\right) \quad (14)$$

Where T is the absolute temperature in Kelvin and  $\mu^* = 5.41 \cdot 10^{-7} Pa.s$  and  $Q = 3570 K$ .

With these parameter values,  $\mu_{TNT} = 11 mPa.s$  at 85°C.

### III.1.2 Solid Phase Characterization

The solid phase is made out of two species: NTO and aluminium. Four batches of NTO, labelled NTO 1, NTO 2, NTO 3, NTO 4 and two batches of aluminium, Al 1, Al 2 are used. They differ by their packing densities and morphologies.

The experimental packing density  $C$  is calculated from the true and bulk densities. The true density  $\rho_t$  is measured with a helium pycnometer from Micromeritics and the true bulk density  $\rho_b$  with a volumenometer.  $C$  is defined by Equation 15:

$$C = \frac{\rho_t}{\rho_b} \quad (15)$$

Average sizes of NTO particles reach 350-400  $\mu m$  and 13  $\mu m$  for aluminium particles. SEM analysis shows spherical morphology for Al 2. Grain morphologies are determined by scanning electron microscopy.

Table 3. NTO and Al experimental packing densities

Batches	$\rho_t (g/cm^3)$	$\rho_b (g/cm^3)$	$C$
NTO 1	1.92	0.99	0.52
NTO 2	1.92	0.97	0.51
NTO 3	1.92	0.75	0.39
NTO 4	1.92	0.79	0.41
Al 1	2.7	1.1	0.41
Al 2	2.7	1.2	0.44

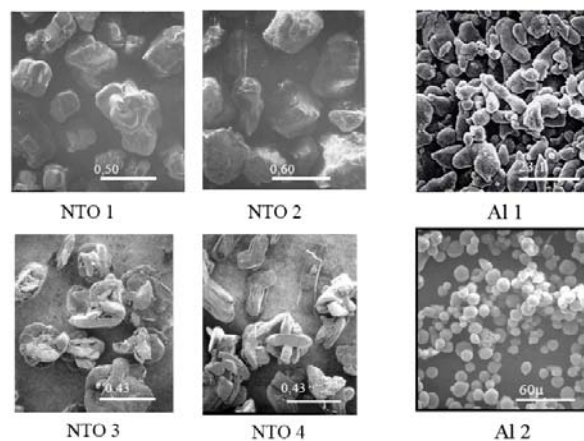


Figure 2. NTO and Al morphologies

### III.2 Experimental Set-Up

Nine insensitive explosive formulations are elaborated with different volume fractions of raw materials. These formulations are given in Table 2. The flow time of 5700 cm<sup>3</sup> of each suspension has been measured and the texture of these energetic pastes has been observed. For the energetic formulations exhibiting a high apparent viscosity, the measurements of the flow time has been made several times to get significant results. The measurement precision decreases when explosive formulations are highly concentrated. In this case, we repeated twice the measurement of the flow time.

As in our industrial process, suspensions flow through a nozzle situated at the bottom of a tank under gravity. The dimensions of the cylindrical tanks are represented on Figure 3.

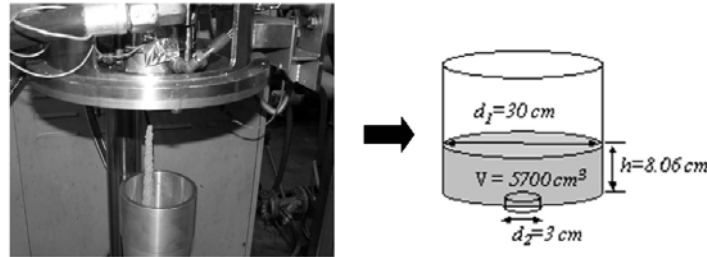


Figure 3. Left: Industrial process; Right, scheme of the tank with some key dimensions

## IV. Results and Discussion

### IV.1 Experimental Results

The flow time and texture of each formulation is reported in the right hand side of Table 2 and depicted on Figure 4. The last formulation (Formulation 9) represents the interstitial fluid, composed of TNT and additive only.

Table 4. Composition and flow time of each insensitive energetic formulation

Formulation	Batche			Volume Fraction $\phi$			$\tau$ (s)
	Al	NTO	TNT	A	Al	NTO	
1	1	2	0.33	0.13	0.09	0.45	72
2	1	1	0.33	0.13	0.09	0.45	168
3	1	3	0.33	0.13	0.09	0.45	720
4	1	3	0.33	0.13	0.09	0.45	1200
5	2	2	0.33	0.13	0.09	0.45	64
6	1	4	0.35	0.14	0.07	0.44	330
7	1	4	0.35	0.14	0.07	0.44	303
8	2	4	0.35	0.14	0.07	0.44	220
9	N/A	N/A	0.72	0.28	0	0	11

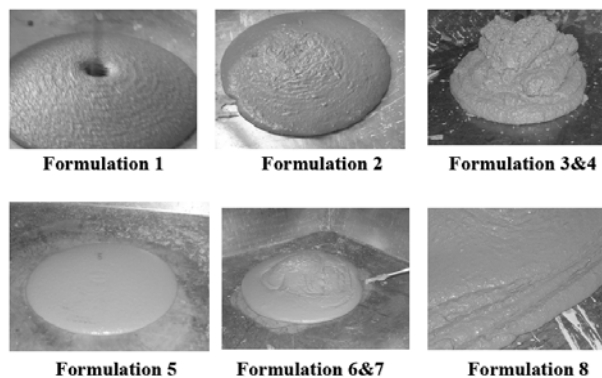


Figure 4. Texture of insensitive energetic pastes

The maximum packing density  $\phi_m$  and the ratio between the maximum packing density and the solid volume fraction  $\phi$  are given in the left hand side of Table 3.

Theoretical flow times are calculated Equations 9, 10 and 11. Final results are listed in the right hand side of Table 3. Results from Equation 10, which are a direct application of Quemada's model, are in agreement with our experimental results.

#### IV.2 Discussion

We assumed that the interstitial fluid can be considered as perfect; this seems to be quite realistic since the experimental flow time (11 s) for 5700 cm<sup>3</sup> corresponds to the theoretical time (13 s) calculated by Equation 8. Moreover, the fair agreement between our experimental results for concentrated suspensions and the theoretical predictions from Quemada's model seems to support our second, intuitive, assumption that the loss of energy due to viscous effects remains negligible. The ratio of the maximum packing density to the solid volume fraction (left hand side of Table 3) gives an interesting information to be compared with the texture of insensitive energetic pastes (Figure 4). When it is close to 1 (Formulations 3 and 4), *i.e.* near the jamming of the structure, the texture is very pasty. On the opposite side, when  $\phi / \phi_m$  decreases (Formulations 1, 2 and 5) or far from 1, energetic pastes present a more liquid behaviour.

*Table 5. Characteristics of each formulation and comparison between theoretical and experimental results*

Formulation	$\phi_m$	$\phi / \phi_m$	$\tau_{theo}$ (s)			$\tau_{exp}$ (s)
			Quémada	Krieger-Dougherty	Mooney	
1	0,79	0,68	128	124	912	72
2	0,79	0,68	128	124	912	168
3	0,61	0,89	972	348	1645790	720
4	0,61	0,89	972	348	1645790	1200
5	0,79	0,68	121	121	815	64
6	0,63	0,81	353	174	10334	330
7	0,63	0,81	353	174	10334	303
8	0,63	0,81	353	174	10334	220
9	0	0	13	13	13	11
R <sup>2</sup>			0,942	0,914	0,910	

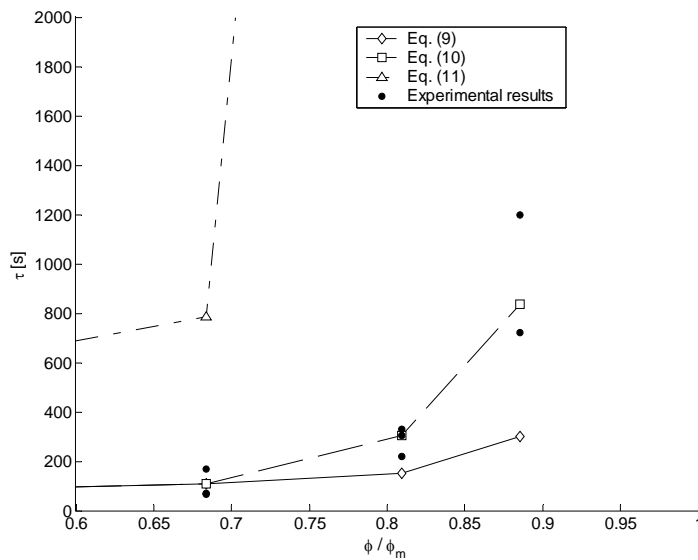


*Figure 5. Comparison between theoretical and experimental results*

As shown on Figure 5, theoretical values of the flow time resulting from Equations 9 and 11 show significant deviations from experimental results. We find that Equation 10 derived from Quemada's model reflects our experimental results more nicely.



## **V. Conclusions**

For suspensions of different formulations, various experiments of casting under gravity have been carried out and the time required by a given volume to pass through a nozzle has been measured. Considering that the suspension flow proceeds under conditions where the inertial term of the Navier-Stokes equation is negligible compared to the viscous term, we find the suspension flow time to be directly proportional to its viscosity. Consequently, the cast time can be calculated from the suspension viscosity. Three models, frequently used in rheology, make possible to calculate this viscosity as a function of the interstitial fluid dynamic viscosity and the ratio  $\phi/\phi_m$  where  $\phi_m$  is calculated with De Larrard's model. The relatively low viscosity of the interstitial fluid allows us to consider perfect fluids and apply the Bernoulli relationship. Comparison between theoretical values and experimental results shows that Quemada's model gives a satisfactory modelling. In the configuration studied, the flow time

can be estimated by the following relationship:  $\tau = \tau_0 \cdot \left(1 - \frac{\phi}{\phi_m}\right)^{-2}$

## **References**

- De Larrard, F., 1967. Formulation et Propriétés des Bétons à très Hautes Performances. Rapport des Laboratoires des Ponts et Chaussées N°149. Thèse de Doctorat de l'Ecole Nationale des Ponts et Chaussées, France.
- De Larrard, F., 1992. A General model for the prediction of voids content in high performance concrete mix design. CANMET/ACI Conference on Advances in Concrete Technology Athens.
- De Larrard, F., C.F. Ferraris, T. Sedran, 1998. Fresh Concrete: Heckel-Bulkley Material. Mater. Struct. 31, 494.
- De Larrard, F., C.F. Ferraris, 1998. Rhéologie du béton frais remanié. II : Relation entre composition et paramètres rhéologiques, N°. 214, REF. 4177. Bulletin des Laboratoires des Ponts et Chaussées, France.
- De Larrard, F., T. Sedran, 2002. Mixture-Proportioning of High-Performance Concrete. Cement and Concrete Research 32, 1699.
- Ferraris, C.F., 1999. Measurement of the Rheological Properties of High Performance Concrete, State of Art Report. J. Res. Natl. Inst. Stand. Technol. 104, 461.
- Gan, M., N. Gopinathan, X. Jia, R.A. Williams, 2004. Predicting Packing Characteristics of Particles of Arbitrary Shapes. KONA 22, 82.
- Krieger, I.M., T.J. Dougherty, 1959. A mechanism for non-Newtonian flow in suspensions of rigid spheres. Trans. Soc. Rheol. 3, 137.
- Mooney, M., 1951. The Viscosity of a Concentrated Suspension of Spherical Particles. J. Colloid Sci. 6, 162.
- Parry, M.A, H.H. Billon, 1988. A Note on the Coefficient of viscosity of pure molten 2,4,6 trinitrotoluene (TNT). Rheol Acta 28, 661.
- Quemada, D., 1977. Rheology of Concentrated Disperse Systems and Minimum Energy Dissipation Principle, I., Viscosity-Concentration Relationship. Rheol. Acta. 16, 82.
- Sedran, T., F. De Larrard, 1994. René-LCPC, Un Logiciel pour Optimiser la Granularité des Matériaux de Génie Civil, Note Technique N°194. Laboratoire des Ponts et Chaussées, France.
- Shilstone, J.M., 1990. Concrete Mixture Optimization. Concret. Int. 12, 33.
- Stovall, T., F. De Larrard, M. Buil, 1986. Linear Packing Density Model of Grain Mixtures. Powder Technol. 48, 1.
- Stroeven, P., M. Stroeven, 2003. Dynamic Computer Simulation of Concrete on Different Levels of the Microstructure- Part 1. Image Anal. Stereol. 22, 1.
- Teipel, U., 2005. Energetic Materials, Particle Processing and Characterization. Wiley-VCH, 43.
- Toutou, Z., C. Lanos, Y. Melingue, N. Roussel, 2004. Modèle de Viscosité Multi-échelle : de la Pâte de Ciment au Micro-béton. Rhéologie 5, 1.